

## Stochastic Polarization Instability in $\text{PbTiO}_3$

K. Datta,<sup>1,\*</sup> I. Margaritescu,<sup>1</sup> D. A. Keen,<sup>2</sup> and B. Mihailova<sup>1</sup>

<sup>1</sup>*Department of Earth Sciences, University of Hamburg, Grindelallee 48, Hamburg—20146, Germany*

<sup>2</sup>*ISIS Facility, Rutherford Appleton Laboratory, Harwell Campus, Didcot, Oxfordshire OX11 0QX, United Kingdom*



(Received 28 March 2018; revised manuscript received 15 August 2018; published 28 September 2018)

Although discussions of structural phase transitions in prototypical ferroelectric systems with the perovskite structure, such as  $\text{BaTiO}_3$  and  $\text{PbTiO}_3$ , started almost seventy years ago, an atomic-level description of the polar characteristics as a function of temperature, pressure, and composition remains topical. Here we provide a novel quantitative description of the temperature-driven local structural correlations in  $\text{PbTiO}_3$  via the development of characteristic relative cationic shifts. The results give new insights into the phase transition beyond those reliant on the long-range order. The ferroelectric-to-paraelectric transition of  $\text{PbTiO}_3$  is realized by the extent of a stochastic polarization instability driven by a progressive misalignment instead of a complete disappearance of the local dipoles, which further suggests that such polarization instability is chemically induced at the morphotropic phase boundary of  $\text{PbTiO}_3$ -based solid solutions with giant piezoelectric effect. As such, our results not only identify the evolving atomistic disorder in a perovskite-based ferroelectric system, but also suggest that polarization instability can serve as a generic fingerprint for phase transitions as well as for better understanding structure-property relationships in  $\text{PbTiO}_3$ -based ferroelectric solid solutions.

DOI: [10.1103/PhysRevLett.121.137602](https://doi.org/10.1103/PhysRevLett.121.137602)

Materials based on  $\text{PbTiO}_3$  (PT) are widely used in modern electronic devices ranging from nonvolatile memories to sensors in aeronautical applications, for which the global market is projected to reach more than 50 billion dollars by 2020 [1]. This is driven by the unparalleled electromechanical properties of PT and its remarkable adaptability to a wide range of chemical doping [2,3]. Moreover, PT has been a prototype throughout the development of phenomenological theories for phase transitions in perovskite-type ferroelectric materials [4–9]. Generally speaking, the success of Landau-type theory and soft-mode concept of phase transitions is supported by the classic behavior of PT, where a nonpolar cubic structure stabilizes a polar tetragonal structure on cooling through ionic displacements with an almost perfect “polarizability catastrophe” phenomenon around the Curie temperature ( $T_C$ ) of 763 K.

However, it is also accepted that the exclusive classification of this phase transition of PT as first-order displacive is not fully correct because the local correlations show substantial order-disorder manifestations [10–14]. The seminal work by Siconolfi *et al.* [12] described the local structural deviations above  $T_C$  using x-ray absorption fine structure (XAFS) spectra revealing that the local and the average structures of PT do not conform to each other well. Since then there has been a number of reports employing different experimental techniques, such as Raman scattering [15], inelastic neutron scattering [16], x-ray single crystal diffraction [10,17–19], as well as XAFS, trying to elucidate the atomic-scale behavior as a function of temperature. Surprisingly though, there is still no precise

description of the sequential development of the atomic arrangement of Pb and Ti through the phase transition. In other words, the overall analytical concepts of the phase transitions may be explicit, but the corresponding physical manifestations remain unclear, with ambiguities such as, how the local structural polarity develops with temperature and to what extent order-disorder processes are coherent with the observed global symmetry changes. These are undoubtedly crucial, not just for improving fundamental understanding of a ferroic phase transition, but more so to derive robust structure-property connections for PT-based solid solutions particularly with composition-driven morphotropic phase boundaries (MPBs), such as  $\text{PbZr}_{0.5}\text{Ti}_{0.5}\text{O}_3$ ,  $x\text{BiScO}_3-(1-x)\text{PbTiO}_3$ , and  $x\text{BiMg}_{0.5}\text{Ti}_{0.5}\text{O}_3-(1-x)\text{PbTiO}_3$ , for which the origin of anomalous physical properties at MPBs are linked to the local structures [20–24].

We present plausible atomistic models of PT as a function of temperature, refined against atomic pair distribution functions (PDFs) obtained from neutron total scattering experiments. We describe the temperature-induced phase transition of PT in terms of intrinsic disorder characterized by relative ionic displacements. It is revealed that the appearance of the paraelectric phase above  $T_C$  can be generically described as the development of a stochastic polarization instability driven by the random order of the local dipoles with reduced correlation lengths. Broadly speaking, beyond their ability to chart the progress of the ferroelectric phase transition in PT, the models can potentially guide us in fingerprinting PT from other analogous systems like  $\text{BaTiO}_3$  [25,26] and further help to reconcile the

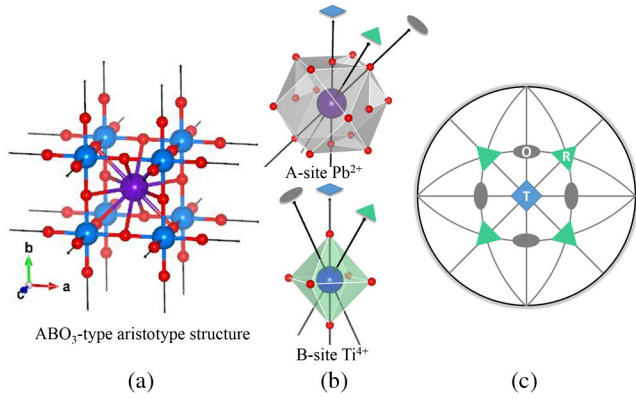


FIG. 1. (a) A schematic of the perovskite-type structure. (b)  $\text{Pb}^{2+}$  is at the A site and  $\text{Ti}^{4+}$  is at the B site with 12 and 6 oxygen neighbors, respectively. (c) A guide stereogram looking down [001] for an ideal cubic crystal with the major pseudocubic directions in the central part from which the symmetry correspondence of the shift directions can be anticipated.

analytical concepts of temperature- and composition-driven phase transitions reported in PT and PT-containing materials.

Neutron total scattering measurements at four different temperatures 300, 500, 700, and 900 K were carried out at ISIS facility in the United Kingdom on the General Materials (GEM) diffractometer [27] using commercially available PT powder (Sigma Aldrich, 99.99%). Data reduction was carried out using the GUDRUN package.

Atomistic model refinements against the experimental PDFs, total scattering functions  $F(Q)$ , and Bragg diffraction pattern used RMCPROFILE software implementation of the reverse Monte Carlo (RMC) technique [28,29]. The RMC configurations consisted of 13 270 atoms in a  $14 \times 14 \times 14$  supercell of the conventional tetragonal or cubic unit cells obtained from the Rietveld refinement of the respective powder pattern. Each RMC iteration was run to generate on average 5000 accepted moves per atom. The refined models were then analyzed using the DISCUS software [30]. At each temperature, there were 40 independent runs to obtain good statistics in the structural parameters. Some additional details on the present analysis are included in the Supplemental Material [31].

PDFs are weighted histograms of all possible atom-atom distances in a given system, and therefore, provide a unique opportunity to investigate the local environments of different atoms [32,38]. Here we have followed the progress of the relative displacements ( $\delta\vec{r}$ ) of each cation as a function of temperature by analyzing their oxygen cages, where in the ideal perovskite structure Pb is at the center of a cuboctahedron, and Ti is at the center of an octahedron (Fig. 1). This method was chosen because the macroscopic properties of a ferroelectric system are mostly governed by the spontaneous polarization ( $P$ ) determined by the relative shifts, plus the shift directions dictate the inherent symmetry of the system [33–35,39,40]. To depict the favored directions of  $\delta\vec{r}$ s, we projected the directions onto

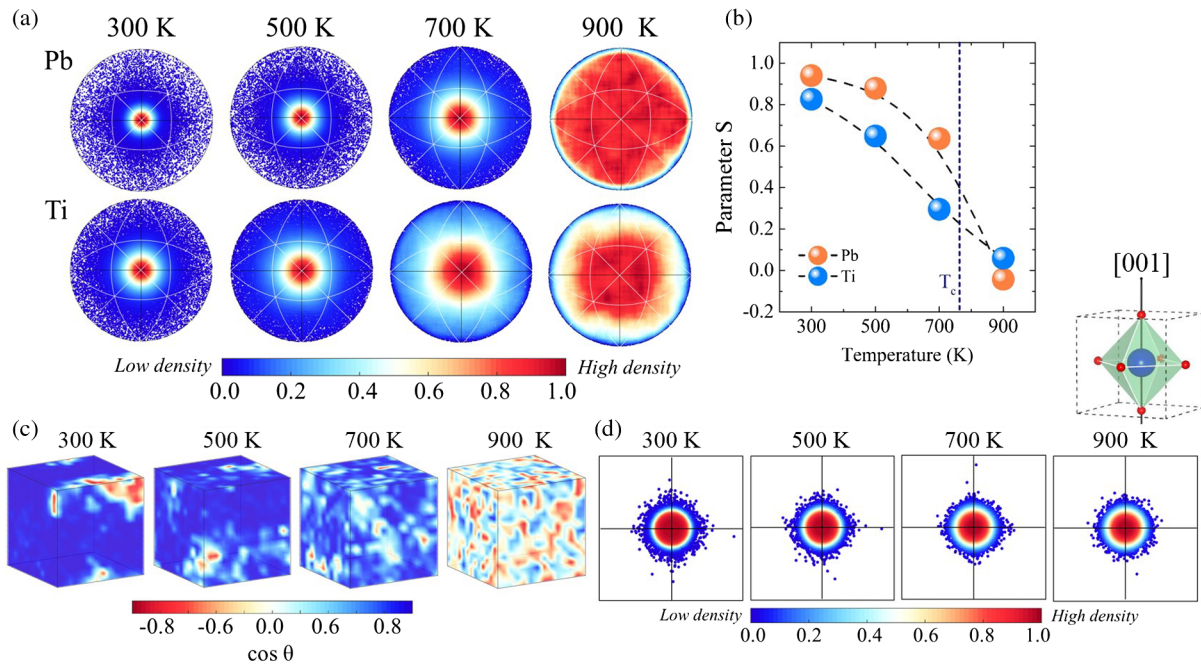


FIG. 2. (a) [001] stereographs with the projected directions of the relative cation displacements. Data from all 40 runs were combined to increase the statistics. (b) Development of  $S$  parameter (see definition in the text) as a function of temperature. The average of  $\cos^2\theta$  at different temperatures was calculated with the point-density values from the respective stereograph as weights. (c) Pseudocolor plots of  $\cos\theta$  of  $\text{Pb}^{2+}$  with their respective unit-cell locations in one of the refined RMC configurations. (e) Stereographs (magnified around [001]) with direction distributions of the [001] apical oxygen atoms of the octahedra. The remaining [010] and [100] stereographs of the corresponding apical oxygen atoms are included in Fig. S9 of the Supplemental Material [31].

stereographs as shown in Fig. 2(a), where the density distributions of the points reflect the preferred displacement directions of the cations with temperature. Clearly, both Pb and Ti have well-defined tetragonal trends at 300 K which progressively disperse at higher temperatures.

An orientational order parameter, defined as

$$S = 1.5\langle \cos^2 \theta \rangle - 0.5 \quad (1)$$

was calculated to quantify this behavior, where  $\theta$  is the angle between [001] (or [00 $\bar{1}$ ]) and  $\delta\vec{r}$ , and lies within  $0^\circ \leq \theta \leq 90^\circ$ . For a perfectly ordered system  $S$  is 1, and  $S$  becomes zero for a highly disordered state with respect to the chosen direction. Therefore, the sequence of  $S$  values in Fig. 2(b) demonstrates how the ordering of Pb and Ti gradually dissipates with the rise of temperature albeit at different rates. Nonetheless the development of  $S$  describing the stereographs reveals a hitherto undetected phenomenon leading to the ferroelectric phase transition of PT, which has been historically explained exclusively via the homogenous deformation of the crystal. Evidently, the paraelectric phase above  $T_C$  is driven by an inherent stochastic polarization instability—a microscopic statistical mechanism—characterized by an ergodic state of local dipoles with random magnitudes and relative orientation. The evolving ergodicity is demonstrated in Fig. 2(d) where we have mapped the values of  $\cos \theta$  ( $0^\circ \leq \theta \leq 180^\circ$  w.r.t. [001]) of the Pb displacements with their respective unit cell location within one of the refined RMC configurations. The spatial fluctuations of the colors within the boxes in Fig. 2(d) reflect the extent of correlation between dipole directions within the simulated crystal and suggest that the local dipoles do not conform to any characteristic pattern with the increase of temperature. In addition, Fig. 2(c) also reminds us the well-known concept of the precursor effect [41] where small polarized clusters increasingly combine in a stochastic fashion on cooling to bring about the ferroelectric ground state below  $T_C$ .

It is important to note that the depicted features of Pb and Ti in Fig. 2(a) are not a secondary phenomenon when compared to the behavior of the oxygen atoms. In fact, the local disorder of oxygen atoms remains almost unchanged in temperature. This has been confirmed by extracting the direction distributions of the apical oxygen atoms of the octahedra with respect to their corresponding pseudocubic axis in stereographs as shown in Fig. 2(d). Consequently, the statistical cation displacements, including any order-disorder event, are not driven by the configurational disorder of oxygen atoms [19].

The temperature dependence of  $\langle |\delta\vec{r}| \rangle$ , derived from the RMC-refined configurations, together with the  $|\delta\vec{r}|$ , calculated from the Rietveld refinements of the neutron powder diffraction, are shown in Fig. 3(a) which essentially depicts the development of the unit-cell polarization with temperature. Trends of shifts clearly indicate the fundamental

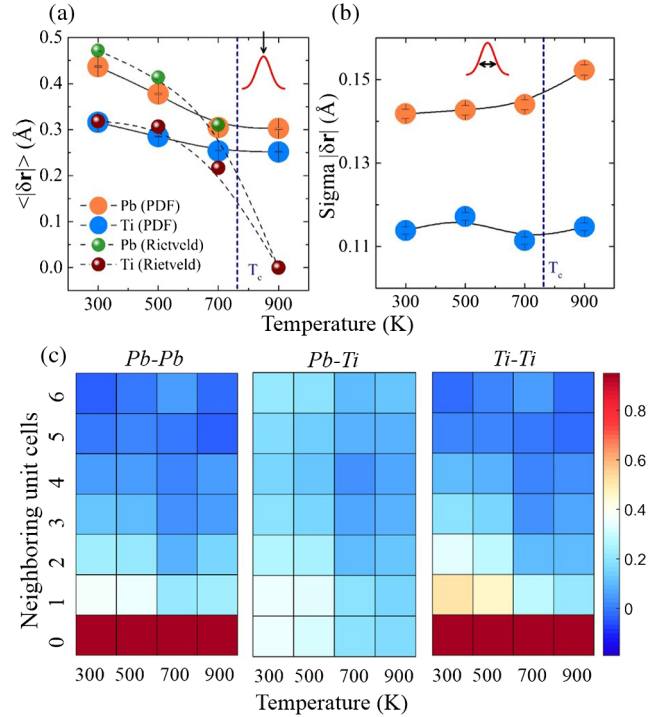


FIG. 3. (a) Development of the mean displacements with temperature. The histograms of the displacement magnitudes are plotted in Fig. S7 of the Supplemental Material [31]. Cation displacements from the Rietveld refinements of the powder diffraction data were obtained assuming a tetragonal ( $P4mm$ ) unit cell throughout the temperature range. (b) Standard deviations of the relative displacements derived from the PDF analyses. (c) Displacement correlation function  $d_{ij}$  for different combinations of cation pairs as functions of temperature and neighbor distances.

basis to classify PT as  $A$ -site-driven ferroelectric which predominantly exhibits a displacive-type phase transition ( $|\delta\vec{r}_{\text{Pb}}| > |\delta\vec{r}_{\text{Ti}}|$ ,  $\forall T$  and  $|\delta\vec{r}|$  is  $T$  dependent). However, the atomic-level displacements are not zero at 900 K, meaning local polarization persists in the paraelectric phase. This is indeed the reason why we observe forbidden first-order Raman scattering for PT above  $T_C$  (Fig. S13 of the Supplemental Material [31]). Moreover,  $\langle |\delta\vec{r}| \rangle$  remains almost constant in the range 700–900 K which suggests that the onset of ferroelectricity in PT at the Curie point is not caused by the formation of dipoles, instead, by an ordering process of already existing dipoles. Or in other words, the onset of paraelectricity above  $T_C$  is not driven by the vanishing spontaneous polarization, rather, it is a consequence of losing the effective dipole-dipole correlations. Hence, locally the structure does not behave in the way expected from the macroscopic Landau-type displacive behavior, where the assumed order parameter ( $P$ ) should be zero in the paraelectric state. Nonetheless the Rietveld-refined structural model above  $T_C$  does have  $|\delta\vec{r}| \approx 0$  [see Fig. 3(a)] and  $\langle |\delta\vec{r}| \rangle$  obtained from the RMC models also tends to be zero in the cubic phase

[see Fig. S8 of the Supplemental Material [31], in contrast to  $\langle |\delta\vec{r}| \rangle$  plotted in Fig. 2(a)].

On the whole, the temperature-induced ferroelectric phase transition in PT can be calibrated by two ingredients: (1) spontaneous dipole moments ( $|\delta\vec{r}|$ ) and (2) inhomogeneities in dipole moments in terms of their relative directions (parameter  $S$ ) and values ( $\sigma(|\delta\vec{r}|)$ ). Evidently, the second phenomenon succeeds the first on heating around the transition temperature and suggests that the so-called order-disorder dynamics sets in as a major phenomenon in the vicinity of  $T_C$ . In fact, this observation corroborates the theoretically derived postulate by Mani *et al.* [42] and several other speculations [10,11,14] that the order-disorder mechanism appears only around the transition point. Evidently the mechanism of the order-disorder phenomenon near the transition point essentially involves a decoupling process of the local dipoles which ultimately brings about the paraelectric phase above  $T_C$ .

In order to substantiate this hypothesis and to gauge the strength as well as the extent of the ferro- or antiferrodistortive coupling within the system, we have calculated a displacement-pair-correlation function  $d_{ij}$  as implemented in the DISCUS package [30]

$$d_{ij} = \langle x_i x_j \rangle / (\langle x_i^2 \rangle \langle x_j^2 \rangle)^{1/2}. \quad (2)$$

Here,  $x_i$  is the displacement of an atom on site  $i$  from the average position in a given direction. A positive  $d_{ij}$  refers to ferrodistorptive correlations, whereas a negative value suggests antiferrodistorptive displacements, and a value around zero signifies the absence of any appreciable correlations, hence random displacements.

The pseudocolor representation of  $d_{ij}$ s in Fig. 3(c), which were calculated along [001]—the macroscopic polar direction of PT—considering all possible pairs of Pb-Pb, Pb-Ti, and Ti-Ti, illustrates the development of the local coupling in different pairs as functions of temperature and neighbor distances. The dominant ferrodistorptive coupling among the cations and their extended presence in the range 300–500 K are evident. Clearly the strength and the extent of the coupling for all pairs go down significantly around 700 K, and interestingly remain very similar up to 900 K. This provides an important corollary that the order-disorder mechanism in fact slackens the nonvisual dynamic correlation among the dipoles, and ultimately gives rise to the paraelectric phase with reduced coherence volume of the switchable dipoles (see also Fig. S10 of the Supplemental Material [31]).

In summary, we provide a novel perspective on the temperature-induced structural phase transition of PT by resolving the development of the atomistic disorder with temperature. At the atomic level the ferroelectric phase transition in PT is fundamentally a stochastic polarization instability-driven phenomenon in which the material finally loses the concerted ferroelectric coupling at  $T_C$ . In other words, the emergence of the ferroelectricity just below the

transition temperature can be seen as a consequence of acquiring the minimum volume of coherent cluster. Furthermore, in relation to the existing empirical concepts of displacive and order-disorder-driven phase transition, we have provided direct and quantitative evidence that PT essentially exhibits characters of both displacive and order-disorder mechanisms; however around the transition temperature order disorder seems to be the driving mechanism which transforms the interacting fluctuations to the non-interacting fluctuations.

In general, it is very interesting to see how the phase transition of a chemically unmodified ferroelectric system can be wholly described by an evolving dielectric instability characterized by parameters like  $S$ ,  $|\delta\vec{r}|$ , and  $\sigma(|\delta\vec{r}|)$ . Surely this provides much fuller understanding on ferro transitions which would be helpful in establishing structure-property relations for functional ferroelectrics. For instance, in the light of similarities in pressure- and temperature- driven ferroelectric-to-paraelectric phase transition in PT, including the hypothesis that elastic stress or electric field can induce or tune an MPB in PT and PT-based systems, analogous to a composition-induced MPB [43–47], it is tempting to assume that the development of underlying atomistic disorder in all cases could be of similar character. As a matter of fact, PT-based solid solutions exhibit similar random polarization instability at the MPBs (Fig. 4) [34–36] where they exhibit anomalously high electromechanical properties in a similar way to PT when it is close to  $T_C$ . In addition, the development of atomic vibrations on approaching  $T_C$  or MPB is equally

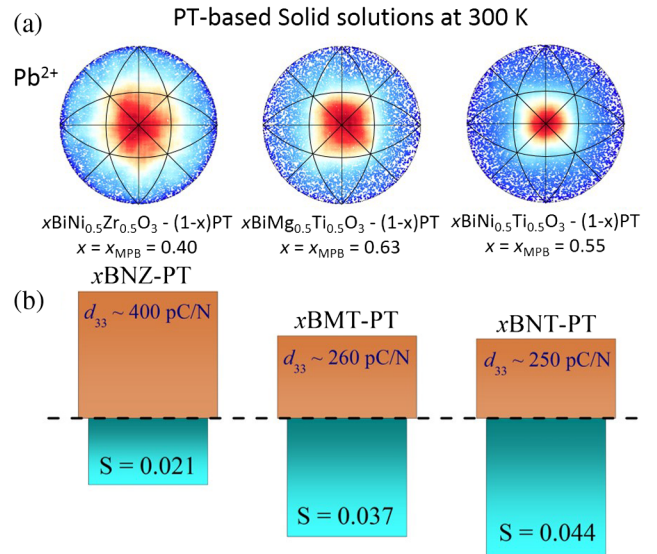


FIG. 4. (a) Apparent similarities in the underlying atomistic disorder seen in stereographs for different PT-based solid solutions with the undoped PT at high temperature. The plots of the solid solutions are redrawn from Refs. [35,36]. (b) Piezoelectric coefficient  $d_{33}$  values of the solid solutions together with the  $S$  parameter suggest that stochastic polarization instability in a ferroelectric system is favorable for better piezoelectric properties.

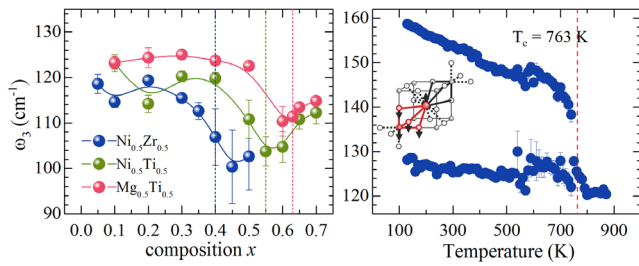


FIG. 5. Ubiquitous softening of  $A-BO_3$  phonon mode ( $T_{1u}$  in  $Pm\bar{3}m$ ) driven by the composition in solid solutions at room temperature [35,36] and the temperature in pure PT [37]. Details on the Raman scattering measurements are included in the Supplemental Material [31].

comparable considering the softening of the  $A-BO_3$  transition phonon mode (Fig. 5), which indicates that the atomistic origin of the MPB properties in PT-based materials is rooted at the high-temperature behavior of the cations, which is virtually mimicked at room temperature by chemical tuning. Hence, we propose that the stochastic polarization instability together with the effective length of interaction in a ferroelectric crystal could be potentially used as a generic fingerprint for phase transitions, and in particular, to predict where elevated physical properties will arise.

Financial support from Deutsche Forschungsgemeinschaft (Grant No. MI 1127/8-2) is gratefully acknowledged. K. D. thanks Reinhard Neder (FAU Erlangen-Nürnberg) for the help in using DISCUS package.

\*kaustuv.datta@uni-hamburg.de

- [1] Innovative Research and Product Inc. Report codes: ET-114, ET-119 and ET-127.
- [2] G. H. Haertling, Ferroelectric ceramics: History and technology, *J. Am. Ceram. Soc.* **82**, 797 (1999).
- [3] K. Uchino, Glory of piezoelectric perovskites, *Sci. Technol. Adv. Mater.* **16**, 046001 (2015).
- [4] A. F. Devonshire, Theory of ferroelectrics, *Adv. Phys.* **3**, 85 (1954).
- [5] W. Cochran, Crystal stability and the theory of ferroelectricity, *Adv. Phys.* **9**, 387 (1960).
- [6] G. Shirane, J. D. Axe, J. Harada, and J. P. Remeika, Soft ferroelectric modes in lead titanate, *Phys. Rev. B* **2**, 155 (1970).
- [7] G. Burns and B. A. Scott, Lattice modes in ferroelectric perovskites:  $PbTiO_3$ , *Phys. Rev. B* **7**, 3088 (1973).
- [8] R. A. Cowley, Structural phase transitions I. Landau theory, *Adv. Phys.* **29**, 1 (1980).
- [9] A. D. Bruce and R. A. Cowley, Structural phase transitions III. Critical dynamics and quasi-elastic scattering, *Adv. Phys.* **29**, 219 (1980).
- [10] R. J. Nelmes, R. O. Piltz, W. F. Kuhs, Z. Tun, and R. Restori, Order-disorder behaviour in the transition of  $PbTiO_3$ , *Ferroelectrics* **108**, 165 (1990).
- [11] M. D. Fontana, H. Idrissi, and K. Wojcik, Displacive to order-disorder crossover in the cubic-tetragonal phase transition of  $PbTiO_3$ , *Europhys. Lett.* **11**, 419 (1990).
- [12] N. Sicron, B. Ravel, Y. Yacoby, E. A. Stern, F. Dogan, and J. J. Rehr, Nature of the ferroelectric phase transition in  $PbTiO_3$ , *Phys. Rev. B* **50**, 13168 (1994).
- [13] K. Sato, T. Miyayaga, S. Ikeda, and D. Diop, XAFS study of local structure change in perovskite titanates, *Phys. Scr.* **2005**, 359 (2005).
- [14] Y.-H. Shin, J.-Y. Son, B.-J. Lee, I. Grinberg, and A. M. Rappe, Order-disorder character of  $PbTiO_3$ , *J. Phys. Condens. Matter* **20**, 015224 (2008).
- [15] J. Hlinka, B. Hehlen, A. Kania, and I. Gregora, Soft mode in cubic  $PbTiO_3$  by hyper-Raman scattering, *Phys. Rev. B* **87**, 064101 (2013).
- [16] I. Tomeno, J. A. Fernandez-Baca, K. J. Marty, K. Oka, and Y. Tsunoda, Simultaneous softening of acoustic and optical modes in cubic  $PbTiO_3$ , *Phys. Rev. B* **86**, 134306 (2012).
- [17] B. D. Chapman, E. A. Stern, S.-W. Han, J. O. Cross, G. T. Seidler, V. Gavrilychenko, R. V. Vedrinskii, and V. L. Kraizman, Diffuse x-ray scattering in perovskite ferroelectrics, *Phys. Rev. B* **71**, 020102 (2005).
- [18] A. Al-Zein, P. Bouvier, A. Kania, C. Levelut, B. Hehlen, V. Nassif, T. C. Hansen, P. Fertey, J. Haines, and J. Rouquette, High pressure single crystal x-ray and neutron powder diffraction study of the ferroelectric-paraelectric phase transition in  $PbTiO_3$ , *J. Phys. D* **48**, 504008 (2015).
- [19] A. Yoshiasa, T. Nakatani, A. Nakatsuka, M. Okube, K. Sugiyama, and T. Mashimo, High-temperature single-crystal X-ray diffraction study of tetragonal and cubic perovskite-type  $PbTiO_3$  phases, *Acta Crystallogr. Sect. B* **72**, 381 (2016).
- [20] H. Fu and R. Cohen, Polarization rotation mechanism for ultrahigh electromechanical response in single-crystal piezoelectrics, *Nature (London)* **403**, 281 (2000).
- [21] D. Damjanovic, Contributions to the piezoelectric effect in ferroelectric single crystals and ceramics, *J. Am. Ceram. Soc.* **88**, 2663 (2005).
- [22] M. Budimir, D. Damjanovic, and N. Setter, Piezoelectric response and free-energy instability in the perovskite crystals  $BaTiO_3$ ,  $PbTiO_3$ , and  $Pb(Zr, Ti)O_3$ , *Phys. Rev. B* **73**, 174106 (2006).
- [23] J. Frantti, Y. Fujioka, J. Zhang, S. C. Vogel, Y. Wang, Y. Zhao, and R. M. Nieminen, The factors behind the morphotropic phase boundary in piezoelectric perovskites, *J. Phys. Chem. B* **113**, 7967 (2009).
- [24] N. Zhang, H. Yokota, A. M. Glazer, D. A. Keen, S. Gorfman, P. A. Thomas, W. Ren, and Z.-G. Ye, Local-scale structures across the morphotropic phase boundary in  $PbZr_{1-x}Ti_xO_3$ , *IUCr* **5**, 73 (2018).
- [25] I. Levin, V. Krayzman, and J. C. Woicik, Local structure in perovskite (Ba, Sr)TiO<sub>3</sub>: Reverse Monte Carlo refinements from multiple measurement techniques, *Phys. Rev. B* **89**, 024106 (2014).
- [26] M. S. Senn, D. A. Keen, T. C. A. Lucas, J. A. Hriljac, and A. L. Goodwin, Emergence of Long-Range Order in  $BaTiO_3$  from Local Symmetry-Breaking Distortions, *Phys. Rev. Lett.* **116**, 207602 (2016).
- [27] P. Day, J. Enderby, W. Williams, L. Chapon, A. Hannon, P. Radaelli, and A. Soper, Scientific reviews: GEM:

- The general materials diffractometer at ISIS-multibank capabilities for studying crystalline and disordered materials, *Neutron News* **15**, 19 (2004).
- [28] R. L. McGreevy, Reverse Monte Carlo modelling, *J. Phys. Condens. Matter* **13**, R877 (2001).
- [29] M. G. Tucker, D. A. Keen, M. T. Dove, A. L. Goodwin, and Q. Hui, RMCprofile: Reverse Monte Carlo for polycrystalline materials, *J. Phys. Condens. Matter* **19**, 335218 (2007).
- [30] R. B. Neder and T. Proffen, *Diffuse Scattering and Defect Structure Simulations: A Cook Book Using the Program DISCUS* (Oxford University Press, Oxford, 2007).
- [31] See Supplemental Material at <http://link.aps.org/supplemental/10.1103/PhysRevLett.121.137602> for additional figures and more details on the adopted methodology for the data analyses, including Refs. [30,32–37].
- [32] D. A. Keen, A comparison of various commonly used correlation functions for describing total scattering, *J. Appl. Crystallogr.* **34**, 172 (2001).
- [33] I. Grinberg, V. Cooper, and A. Rappe, Relationship between local structure and phase transitions of a disordered solid solution, *Nature (London)* **419**, 909 (2002).
- [34] K. Datta, A. Richter, M. Göbbels, D. A. Keen, and R. B. Neder, Direct mapping of microscopic polarization in ferroelectric  $x(\text{BiScO}_3) - (1-x)\text{PbTiO}_3$  throughout its morphotropic phase boundary, *Phys. Rev. B* **93**, 064102 (2016).
- [35] K. Datta, R. B. Neder, J. Chen, J. C. Neuefeind, and B. Mihailova, Atomic-level structural correlations across the morphotropic phase boundary of a ferroelectric solid solution:  $x\text{BiMg}_{1/2}\text{Ti}_{1/2}\text{O}_3 - (1-x)\text{PbTiO}_3$ , *Sci. Rep.* **7**, 471 (2017).
- [36] K. Datta, R. B. Neder, J. Chen, J. C. Neuefeind, and B. Mihailova, Favorable Concurrence of Static and Dynamic Phenomena at the Morphotropic Phase Boundary of  $x\text{BiNi}_{0.5}\text{Zr}_{0.5}\text{O}_3 - (1-x)\text{PbTiO}_3$ , *Phys. Rev. Lett.* **119**, 207604 (2017).
- [37] I. Margaritescu, K. Datta, and B. Mihailova, Multistep coupling of preexisting local ferroic distortions in  $\text{PbTiO}_3$  above the Curie temperature, *J. Phys. Condens. Matter*, 10.1088/1361-648X/aae344 (2018).
- [38] T. Egami and S. Billinge, *Underneath the Bragg Peaks Structural Analysis of Complex Materials* (Pergamon Materials Series, Oxford, 2012).
- [39] R. Resta, Macroscopic polarization in crystalline dielectrics: the geometric phase approach, *Rev. Mod. Phys.* **66**, 899 (1994).
- [40] N. Zhang, H. Yokota, A. M. Glazer, Z. Ren, D. A. Keen, D. S. Keeble, P. A. Thomas, and Z.-G. Ye, The missing boundary in the phase diagram of  $\text{PbZr}_{1-x}\text{Ti}_x\text{O}_3$ , *Nat. Commun.* **5**, 5231 (2014).
- [41] A. Bussmann-Holder, H. Beige, and G. Völkel, Precursor effects, broken local symmetry, and coexistence of order-disorder and displacive dynamics in perovskite ferroelectrics, *Phys. Rev. B* **79**, 184111 (2009).
- [42] B. K. Mani, C.-M. Chang, and I. Ponomareva, Atomistic study of soft-mode dynamics in  $\text{PbTiO}_3$ , *Phys. Rev. B* **88**, 064306 (2013).
- [43] Z. Wu and R. E. Cohen, Pressure-Induced Anomalous Phase Transitions and Colossal Enhancement of Piezoelectricity in  $\text{PbTiO}_3$ , *Phys. Rev. Lett.* **95**, 037601 (2005).
- [44] M. Ahart, M. Somayazulu, R. E. Cohen, P. Ganesh, P. Dera, H.-k. Mao, R. J. Hemley, Y. Ren, P. Liermann, and Z. Wu, Origin of morphotropic phase boundaries in ferroelectrics, *Nature (London)* **451**, 545 (2008).
- [45] P.-E. Janolin, P. Bouvier, J. Kreisel, P. A. Thomas, I. A. Kornev, L. Bellaiche, W. Crichton, M. Hanfland, and B. Dkhil, High-Pressure Effect on  $\text{PbTiO}_3$ : An investigation by Raman and x-ray Scattering up to 63 GPa, *Phys. Rev. Lett.* **101**, 237601 (2008).
- [46] J. Rouquette, J. Haines, V. Bornand, M. Pintard, Ph. Papet, C. Bousquet, L. Konczewicz, F. A. Gorelli, and S. Hull, Pressure tuning of the morphotropic phase boundary in piezoelectric lead zirconate titanate, *Phys. Rev. B* **70**, 014108 (2004).
- [47] M. Hinterstein, J. Rouquette, J. Haines, Ph. Papet, M. Knapp, J. Glaum, and H. Fuess, Structural Description of the Macroscopic Piezo- and Ferroelectric Properties of Lead Zirconate Titanate, *Phys. Rev. Lett.* **107**, 077602 (2011).